TUTORIAL ON LOW BETA CAVITY DESIGN

A. Facco, INFN – LNL

Abstract

Low beta superconducting cavities are gaining more and more interest in the particle accelerators community. Their use, once limited to low current, low energy heavy ion beams, was recently extended to high current proton and deuteron linacs for energy production, spallation neutron sources, radioactive beam production, nuclear waste transmutation and other applications.

A large number of different resonator geometries is now available, with peculiar characteristics suitable for different applications. In spite of their complex structures and construction difficulties, their performance, in terms of surface resistance and maximum achievable electric and magnetic fields, is comparable to the one of high gradient elliptical cavities.

An introduction on low-beta resonators types, characteristics and design techniques, including accessories which are typical of this class of cavities, will be given.

1. INTRODUCTION

Low-β resonators are just cavities that accelerate efficiently particles with velocity β<1. This set is usually further subdivided in low-, medium- and high-β ones, centered around β=0.1 in linac boosters for Tandem accelerators, and around β=0.3÷0.6 in all other SC linacs communities.

Differently from β=1 cavities, that have all elliptical-like profiles (see, e.g. ref. [1]), low-β ones have many different shapes, sizes and EM modes to allow for a rather large variety of beams that differ in velocity, intensity and A/q. Important differences are also the higher peak surface fields E_p and B_p required to get the same acceleration, and the lower rf frequency.

A typical Superconducting low-β linac consists of many short cavities, independently powered and phased (ISCL), with a small number of gaps (typically 2 or 3) and relatively large aperture compared to normal conducting ones. This structure allows a large velocity acceptance, different beam velocity profiles along the linac and thus the capability of accelerating efficiently particles with different A/q. Moreover, this allows to some extent linac lattices with cavity fault tolerance.

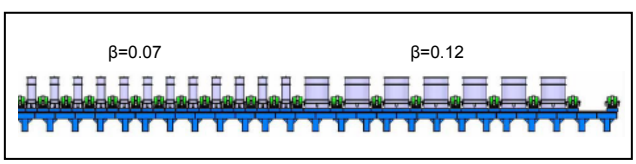

Figure 1. Example of low-β SC linac scheme: the SPIRAL-2 driver (GANIL), with cryostats housing 1- and 2- double gap cavities each.

The first superconducting low-β resonators have been used from the 70's in linac boosters for tandem accelerators. The low current, cw heavy ion beams produced by tandems, with wide range of mass to charge ratio and 0.05≤β≤0.2, were an ideal application for superconducting structures with 2÷3 gap, that could be powered with a few tens of Watts only.

In the last decade, however, an important boost to low-β cavity development was given by R&D programs on high intensity proton and ion drivers for nuclear waste transmutation, material irradiation, accelerator driven reactors, radioactive beam production and post-acceleration, and other applications (see table 1). This extended the resonator families and also their performance.

Type	β_{max}	A/q	current mA
Heavy ion linacs for nuclear physics	~ 0.2	<10	$< 10^{-4}$
Post-accelerators for RIB facilities	~ 0.2 (0.5)	7÷ 66	$< 10^{-6}$
HI drivers for RIB facilities	~ 0.3÷0.9	~1÷10	~0.1÷10
p,*d* linacs	~ 0.3	1 ÷ 2	~1÷10
High Power Proton Accelerators	~ 0.9	1	~10÷100
High Power Deuteron Accelerators for material irradiation	~ 0.3	2	~100

Table 1. Low-β resonator applications.

2. BASIC DEFINITIONS

For tutorial purposes, in this introductory paper we will use beam dynamics and rf formulas in their simplest form. For a deeper understanding and a more general approach see ref. [2] and [3].

A resonator working in its accelerating mode has a time dependent electromagnetic field of the form

$$\vec{E} = \vec{E}(x,y,z)\cos(\omega t + \varphi)$$

$$\vec{B} = \vec{B}(x,y,z)\sin(\omega t + \varphi)$$

To characterize superconducting resonators, parameters are used that relate their measurable rf and

electromagnetic characteristics. Some of the most important ones are shown in Table 1. All parameters in the table are constants that depend on the cavity geometry, surface resistance and accelerating field [4][5].

Stored energy	U/E_a^2	$J/(MV/m)^2$
Shunt impedance	$R_{sh}=E_a^2L/P$	$M\Omega/m$
Quality Factor	$Q=\omega U/P$	
Geometrical factor	$\Gamma = Q\,R_s$	Ω
Peak electric field	E_p/E_a	
Peak magnetic field	B_p/E_a	$mT/(MV/m)$
Optimum β	β_0	
Cavity length	L	m

Table 2. Main parameters that characterize a superconducting cavity.

Here:
$\omega = 2\pi f$ rf frequency
E_a =Average accelerating field (MV/m)
P =rf power losses in the cavity (W), proportional to R_s
$R_s = R_{BCS} + R_{RES}$ surface resistance of cavity walls Ω.

The residual resistance R_{RES} depends on the quality and purity of the rf surface.

R_{BCS} is the theoretical value for pure Nb:

$$R_{BCS}(n\Omega) \cong 0.09 \cdot \frac{f^2(MHz)}{T(K)} \cdot \exp\left(-\frac{17.67}{T}\right) \quad (1)$$

The accelerating field on the beam axis is usually axially symmetric and can be expressed by

$E_z(r,z,t)=E_z(r,z)\cos(\omega t+\varphi)$

(For simplicity, we assume to be on axis, so that r=0, and $E_z(0,z) \equiv E_z(z)$).

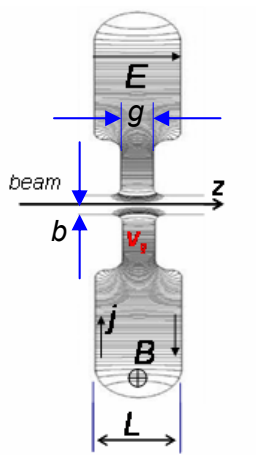

Figure 2. 1-gap resonator schematic and definitions.

We can define the average accelerating field

$$E_a = \frac{1}{L}\int_{-L/2}^{L/2} E_z(z)dz \quad (2)$$

In this definition, E_aL is the maximum gap voltage V_g.

A particle traversing the cavity with velocity βc, charge q and coordinate z_p, however, has always an energy gain ΔW_p lower than qV_g, due to the change in the field during the finite time of transit.

$$\Delta W_p = q\int_{-L/2}^{L/2} E_z(z_p,t)dz_p \quad (3)$$

Using the constant velocity approximation, and choosing $t=0$ when the particle crosses $z=0$, then $t=z_p/\beta c$ and the instantaneous accelerating field becomes $E_z(z_p)\cos(\omega z_p/\beta c+\varphi)$. Introducing the transit time factor

$$T(\beta) = \frac{\int_{-L/2}^{L/2} E_z(z)\cos\left(\frac{\omega z}{\beta c}\right)dz}{\int_{-L/2}^{L/2} E_z(z)dz} \le 1 \quad (4)$$

we obtain the usual expression for the energy gain:

$$\Delta W_p = qE_aLT(\beta)\cos\varphi \quad (5)$$

The transit time factor for 1 gap of length g is particularly simple in the approximation of constant E_z in the gap and zero outside:

$$T(\beta) = \frac{\sin\left(\frac{\pi g}{\beta\lambda}\right)}{\left(\frac{\pi g}{\beta\lambda}\right)} \equiv \frac{\sin\left(\frac{\pi g f}{\beta c}\right)}{\left(\frac{\pi g f}{\beta c}\right)} \quad (6)$$

The real field in the gap, however, is not constant and the beam port aperture allows the field to extend beyond g. This results in an "effective gap length" larger than g, approximately $g_{eff} \approx \sqrt{g^2+(2b)^2}$ where b is the bore radius.

An example of a 1 gap transit time factor, using two different aperture values, is shown in figure 3.

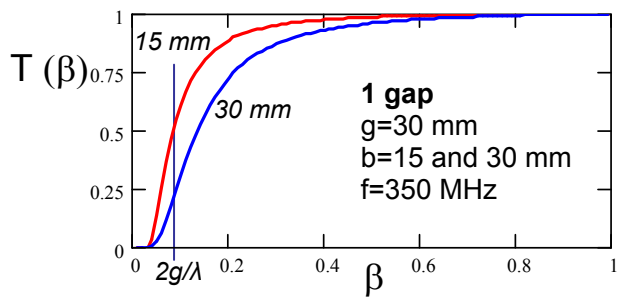

Figure 3. Single-gap transit time factor curves, for the same gap length and different apertures.

Acceleration takes place efficiently only above some critical $\beta_0 \sim 2g_{eff}/\lambda$ and it is maximum at $\beta=1$. Thus, to be efficient at low-β, it is necessary to work at low rf frequency, short gap length and small beam port aperture. Rules of thumb for a good design are: $2gf<\beta c$ and $2b<g$.

For 2 equal gaps at a distance d, working in the usual π-mode (i.e. where there is a phase delay of π between the EM field in the two gaps) we have:

$$T(\beta)=\frac{\sin\left(\frac{\pi g}{\beta\lambda}\right)}{\left(\frac{\pi g}{\beta\lambda}\right)}\sin\left(\frac{\pi d}{\beta\lambda}\right) \qquad (7)$$

In general, for a resonator with 2 or more equal gaps, $T(\beta)$ consists of the single gap term plus a term accounting for the sinchronization of the field with the particle phase in different gaps. In this case, T has a maximum $T(\beta_0)<1$ at some optimum velocity $\beta_0<1$.

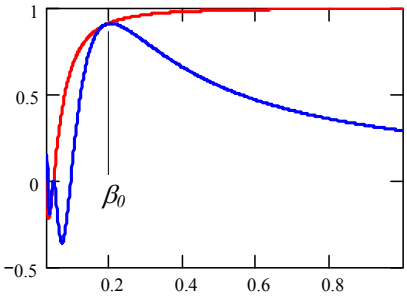

Figure 4. Example of transit time factor for a 2-gap resonator (π-mode). Red curve: 1-gap term; blue curve: total $T(\beta)$.

It is usually better to normalize the transit time factor and the accelerating field expressions:

$$T^*(\beta)=\frac{T(\beta)}{T(\beta_0)} \qquad (8)$$

$$E^*_a=\frac{T(\beta_0)}{L}\int_{-L/2}^{L/2}E_z(z)dz \qquad (9)$$

Thus $T^*(\beta_0)=1$, and E^*_a is not anymore the gap voltage but the real field seen by the particle at optimum β and φ. (From now on we will use normalized quantities and we will omit the asterisk). The energy gain expression (5) does not change.

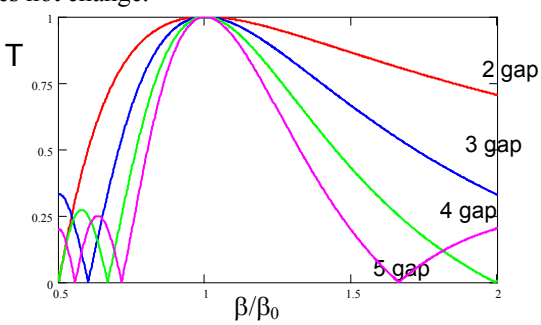

Figure 5. Normalized transit time factor curves vs. normalized velocity β/β_0, for cavities with different number of equal gaps.

Of course, the larger the number of gap of a resonator, the larger is the energy gain that we can expect, but the narrower the velocity acceptance (figure 5).

The requirements of low-β cavities carry some negative consequences. Short gaps provide little energy gain; low rf frequency results in large resonators or complicated shapes; small aperture means low transverse acceptance for the beam. All these items result in cavities with rather high peak-to-accelerating field ratios.

Superconducting resonators are particularly suitable for counteracting these drawbacks, thanks to their low power dissipation and the high surface fields that they can achieve. Due to the low frequency, the surface resistance in equation (1) is rather low already at 4.2K; differently from most β=1 ones, low-β cavities usually do not need to be cooled below this temperature.

Remark: different definitions of gradient

The resonator performance is usually represented in a Q vs. E_a plot. With the many different shapes and geometries available for low beta cavities, it is sometimes difficult to find a unique definition of the effective length L which appears in the average gradient expression. The most used definitions are (see figure 6) l_{int} , L_{max} or even $n\beta\lambda/2$, where n is the gap number.

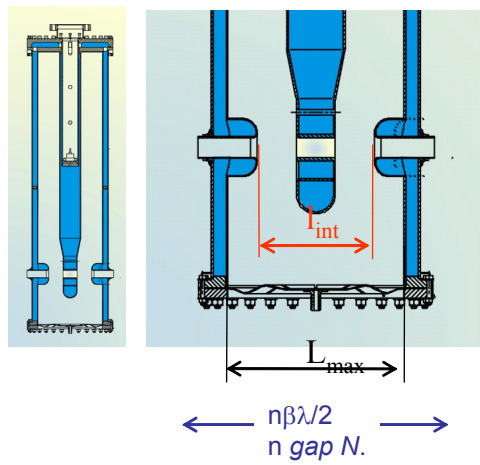

Figure 6. Different definitions of accelerating length in a 2-gap quarter wave resonator.

All definitions are consistent and the energy gain of a resonator has of course always the same value with all of them. However, the shorter L is defined, the larger E_a appears in the graph; the discrepancy can be rather large especially in 1 and 2 gap resonators. Thus, when comparing gradient in different resonators, it is important to know how the cavity lengths are defined.

3. LOW-β CAVITIES DESIGN

A good SC low-β resonator must fulfil the following principal requirements:

- large energy gain
- large shunt impedance (thus low power dissipation)
- easy and reliable operation
- easy installation and maintenance
- low cost-to-performance ratio

The main specifications determining the initial cavity design characteristics derive from the beam.

beam energy	→	β_0, gap length
velocity acceptance	→	n. of gaps
beam size, transv.	→	bore radius
beam long. size & freq.	→	rf frequency
beam power	→	rf coupling type
cw or pulsed	→	mech. Design

Other technical choices in the cavities (thus in the linac) can be prompted by requirements on budget, space, flexibility, availability, fault tolerance, and by other aspects that sometimes make a less performing resonator a better choice for a successful project.

Resonators technology

The available resonator technologies are substantially three.

1. **Bulk Nb** (by far the most used)

Resonators are made of full niobium with high RRR (150÷300); sometimes they include, as part of the structure, a He vessel made of normal grade niobium or stainless steel. The resonator parts are obtained by machining Nb sheets, rods, plates,etc., and are joined together by electron beam welding in high vacuum. Even rather complicated shapes can be obtained with this technology, which is well mastered by industry and allows the highest performance. The surface treatment techniques developed for electron cavities (chemical polishing, electropolishing, high pressure water rinsing etc.) have been fully transferred to low-β ones with excellent results.

2. **Sputtered Nb on Cu** (mostly at INFN-Legnaro[6])

The resonator is made of thick OFHC Copper, possibly with no brazing, with rounded shape optimized for sputtering and no holes in the high current regions. A thin layer of Nb (~1÷2 μm) is deposited on its rf surface by sputtering. This allows to merge the excellent thermal properties of OFHC Copper and the superconducting ones of the Nb. Compared to bulk Nb ones, sputtered cavities not always have comparable performance but can allow cost savings, especially for large production. This technology is well suited for regular geometries, with large openings for cathode insertion and large volumes to maintain sufficient distance between cathode and cavity walls. Until now, sputtering was fully exploited in low-β cavities at INFN Legnaro on 160 Mhz quarter-wave resonators, but R&D is going on to extend the technique to other kinds of resonators like RFQs.

3. **Pb platet on Cu** (in some tandem boosters)

OFHC Copper resonators are plated with Pb by means of electrochemical processes. Compared to the previous case, this older technique has lower cost, can be performed in-house with minimum equipment and can be applied to a larger variety of geometries. The superconducting properties of Pb, however, are not comparable to the ones of Nb; this results in significantly lower gradients (less than 50%).

The first low-β superconducting linacs have been made this way, and some of them are still in operation. The Pb technology is being replaced with the Nb one.

Resonators performance limitations

Performance limitations in low-β superconducting resonators are similar to the ones of β=1 cavities, with some peculiarities generated by low frequency and different geometry.

Critical surface properties. The present achievements in critical surface properties of low-β superconducting cavities, in laboratory test and in operation, are shown in table 3. These results seem not to depend too much on resonator frequency and shape.

	Symbol	achieved	reliable spec.
Max. surface electric field	E_p(MV/m)	~60	30÷35
Max. surface magnetic field	B_p (mT)	~120	60÷70
Residual surface resistance	R_{res}(n Ω)	~1	5÷10

Table 3. Critical surface properties reported for Niobium low-β resonators and values reliably achieved in operation.

Q-slope. The so-called Q-slope is observed in almost all high-Q low-β resonators, where it usually shows a roughly exponential behavior (a straight line in the logarithmic plot for Q, see figure 9). Differently from the Q decay originated by field emission, this effect is not associated with production of x-rays and cannot be reduced by rf conditioning. The Q-slope is not yet completely understood [21][22][23]. It gives an important dependence of the surface resistance R_s on accelerating field, that must be taken into account in resonator design specifications at high field.

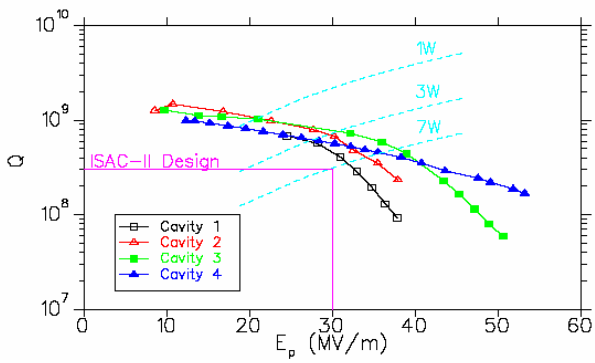

Figure 9. Q-slope in high-Q quarter-wave resonators. Cavity 4 shows a pure Q-slope behaviour. Cavities 1,2 and 3 show also typical field emission behavior at high field, that can be usually eliminated by rf conditioning.

Q-disease. Q disease [4] affects also low-β cavities. In low frequency ones it has been observed only recently. It causes a strong reduction of Q in Nb resonators with large bulk hydrogen concentration, when they are kept for a long time in the 150>T>60 temperature range during cooldown. The Q can be fully recovered by heating the cavity above 150 K and then applying a fast cooldown (tens of minutes, the shorter the better). Large bulk hydrogen concentration can be avoided with a careful

cavity construction and chemical polishing, but not in electropolished cavities (a definitive cure, if necessary, is elimination of the hydrogen by baking the resonator at 700÷900 °C). To avoid problems, fast resonator cooling in the dangerous range of temperatures should be foreseen at the design stage.

Multipacting (MP) is the resonant field emission of electrons from the cavity walls [4]. It sets up under the following conditions:

- stable electron trajectories ending on cavity walls
- electron time of flight multiple of ½ rf cycle (the multiplicity order depends on the particular MP trajectory)
- secondary electron emission coefficient δ >1
- presence of an initial electron impinging the right surface at the right field and phase intervals, to start the process.

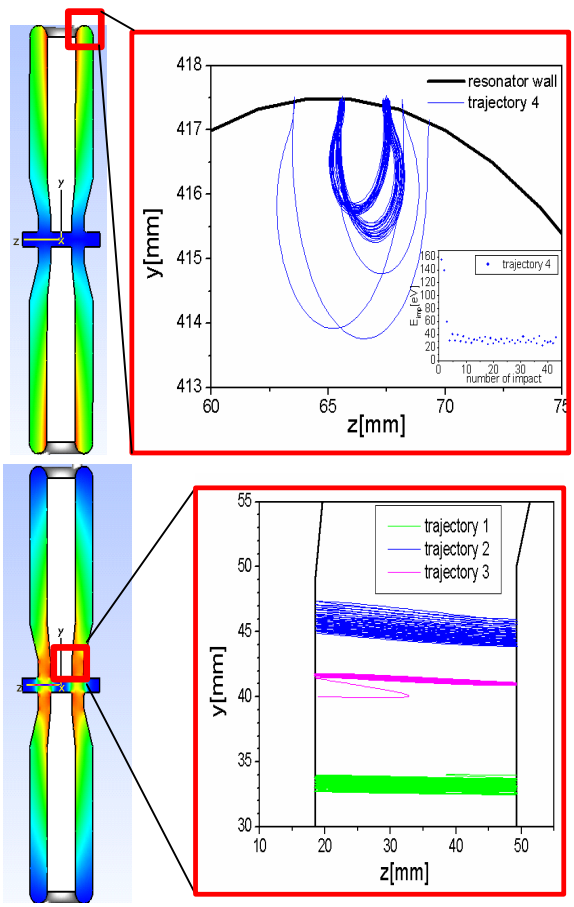

Figure 7. MP in a half–wave resonator. Top: 1-wall "horseshoe" MP in a high magnetic field region. Bottom: 2-walls MP in a high E field (courtesy of ACCEL).

Multipacting is almost impossible to avoid in low-β cavities, due to the presence of involute geometries. Most resonators, however, show only multipacting levels at low gradient, that can be conditioned with low rf power in a reasonable time (up to about one day).

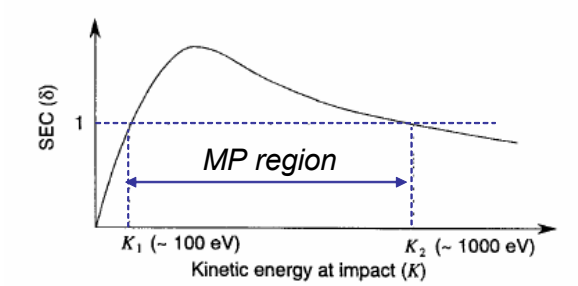

Figure 8. Qualitative graph of the secondary electron emission coefficient in Nb.

Resonator design

As in the high-β case, the resonator design requires a sequence of steps and includes electromagnetic, mechanical and thermal aspects, as well as beam dynamics ones that must be integrated together. This involves the use of different simulation codes and different design skills.

EM design. This requires the design of the cavity geometry with the specified frequency, modes and mechanical constraints. Its optimization includes:

1. minimization of the peak surface fields E_p/E_a and B_p/E_a;
2. maximization the shunt impedance $E_a^2/(P/L)$;
3. optimization the fields for beam dynamics;
4. optimization of the geometry for elimination of multipacting;
5. positioning of apertures suitable for rf coupling and for resonator cleaning.
6. Positioning of a suitable tuning section in the resonator walls.

Rf coupling. Inductive couplers are used for low rf power applications (<1 kW) and low f (<300 MHz); there is sufficient experience in these devices. For high-power, medium- and high-β elliptical cavities, successful capacitive couplers are also available [7]. There are only a few examples, however, of couplers designed for high power low-β cavities. These couplers can be larger than resonators and require a well integrated design [8]. The know-how developed for electron cavities can be fruitfully used for low-β ones.

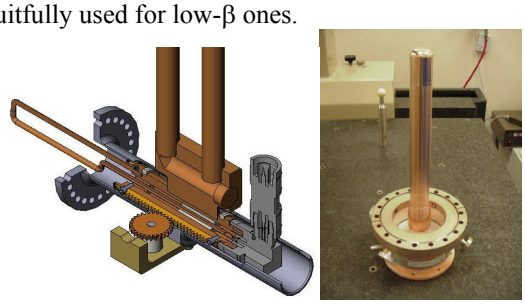

Figure 10. Low-power inductive and high-power capacitive couplers (not in the same scale).

Beam steering. Non symmetric cavities can have non-symmetric EM fields in the beam region. This can produce undesirable beam steering .

The magnetic field gives usually the dominant contribution especially in quarter-wave resonators (QWRs) with large aspect ratio (i.e. approximately for $\beta_0 \cong L/\lambda > 0.1$); this can give serious beam dynamics problems, especially for high intensity beams. QWRs working above ~100 MHz often need some correction.

Using the approximation of constant field in the gap, the vertical kick in a QWR can be represented as follows:

$$\Delta y' = \frac{qE_a LT(\beta)}{\beta\gamma mc^2}\sin\varphi\left(\frac{K_{EY}}{\beta\cdot tg\left(\frac{\pi d}{\beta\lambda}\right)} - cK_{BX}\right) \qquad (10)$$

where $K_{EY}=|E_y/E_z|$ and $K_{BX}=|B_x/E_z|$, calculated in one gap.

During acceleration, for typical values of φ ~20÷30 deg, E_y is symmetric and tends to cancel in the 2 gap (see figure 11), while B_x is antisymmetric and adds up, becoming dominant. Steering is proportional to $qE_aLT(\beta)\sin\varphi$: this expression is rather similar to the rf defocusing effect in misaligned cavities, proportional to $qE_aLT(\beta)\sin\varphi \cdot r$, where r is the displacement of the beam axis from the beam port axis.

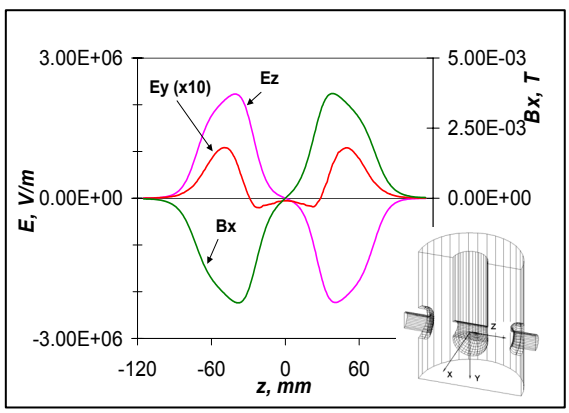

Figure 11. Profiles of the accelerating field and of the steering E_y and B_x components in a QWR.

In low-β QWRs with small aspect ratio, a slight misalignment, if properly done, is usually sufficient to cancel most of the steering thanks to rf defocusing. In cavities where the required misalignment would become too large compared to the beam port aperture, compensation can be obtained by gap shaping: the magnetic deflection can be cancelled by an artificial enhancement of the electric deflection [11] (see fig. 12).

Higher order modes. In high power pulsed linacs, higher order modes should be also considered; at present, only multi-cell elliptical cavities with β>0.6 are used in such conditions and the techniques developed for β=1 cavities, like higher order mode dampers, can be applied [12].

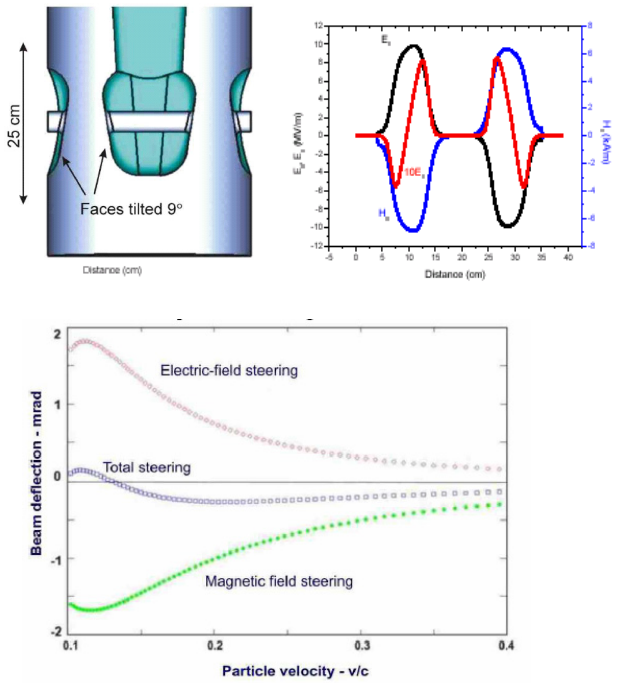

Figure 12. Steering correction by drift tube shaping in QWRs.

Multipacting must be also considered in cavity design. Computer simulation codes can be used for shaping the cavity in order to avoid stable MP trajectories with electron impact energy in of the δ>1 region. Lack of symmetry of most low-β geometries often requires three-dimensional codes and very long computing time. Lack of symmetry, however, also prevents MP to extend to too large areas: old low-β cavities, even if designed with no possibility of MP simulations, have almost always been made to work with reasonable conditioning time.

Rf power losses calculations are required to maximize cavity shunt impedance. The maximum rf power density on the cavity wall should be kept below ~1 W/cm^2 at 4.2K, to allow efficient heat removal by liquid Helium [4]. A large safety margin is required in operation conditions, since local defects can increase power losses significantly and cause cavity quench.

The **mechanical design** can be performed with standard techniques using the powerful codes which are commercially available. The procedure includes:

- Statical analysis (stability against He pressure, radiation pressure, mechanical tuning, …)
- Dynamical analysis (mechanical modes…)
- Thermal analysis (cooling, T distributions,…)
- Construction procedure.

The thermal conductivity at 4.2 K is k=RRR/4 (W/m)/K. Thus high RRR Nb material is required, which has poorer mechanical properties compared to normal grade Nb (RRR~40), and higher cost. A typical good choice for rf cavities is RRR~200÷300. Accumulation of He gas bubbles on the cavity walls can limit heat

exchange on the Nb-He interface. Good ways for liquid He transport and for gas He removal must be provided: this can be rather complicated in low-β geometries, sometimes requiring forced He flow, syphons and other accessories.

Low-power density surfaces (e.g. tuning plates) can be cooled by He gas and by thermal conduction through rf joints, where experience made in many laboratories suggests not to exceed a few mT magnetic field. The effect of a possible super- to normal-conducting transition in such regions should be checked: sometimes it is not critical for cavity operation and low quality plates can be used without problems.

Tuning and mechanical instabilities. Mechanical tuning requires cavity deformation. Wall displacement toward high electric (magnetic) field areas cause rf frequency decrease (increase). Many designs are available for slow tuning that use motors (inside and/or outside cryostats). The same mechanisms cause cavity detuning in the presence of mechanical noise and undesired forces acting on the cavity walls.

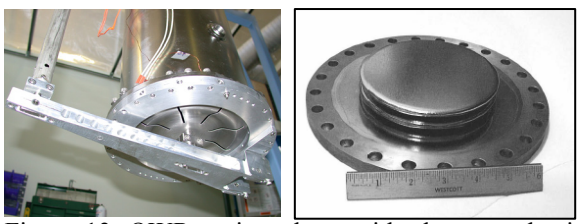

Figure 13. QWR tuning plates with electromechanical (left, TRIUMF design) and gas pressure actuation (right, ANL design).

Cavity detuning around the center frequency is proportional to He pressure changes: $\delta f \propto \delta P$. The effect on cavity ability to maintain the operating conditions depend on the resonator bandwidth and rf system capabilities.

Cu-Pb and Cu-Nb QWRs with thick walls are rather insensitive to pressure variation. For Nb low-β cavities, typical *df/dP* values are from a few to a few tens of Hz/mbar. A good mechanical design can reduce drastically these values. Mechanical tuners can be used for slow frequency compensation in feedback with the frequency error, and the cryogenic system should be carefully designed with sufficient pressure stability.

Source:	***Solution:***
Helium pressure variations	mechanical tuning in feedback, mechanical strengthening
Lorentz Force detuning	slow tuning and rf feedback
microphonics	fast tuners, mechanical design, noise shielding, etc.
resonant vibrations	mechanical damping

Table 4. Mechanical instabilities sources and cures.

Since it is impossible to eliminate completely deformations caused by He pressure fluctuations, the resonator can be designed in order to produce displacements with opposite effects to the frequency, to obtain a balance. Double wall structures allow to null the net force on cavity walls and allow to expose large surfaces to He pressure without making them collapse.

A clever "self-compensating" resonator design, where every displacement in high *E* region is associated in an equivalent one in a high *B* region, can keep df/dP close to zero [13].

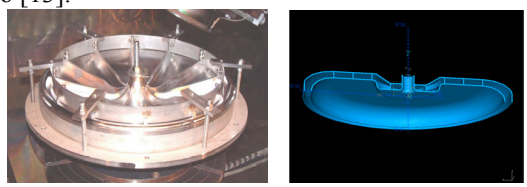

Figure 14. (Left) SPOKE cavity end plate with "self-compensating" design obtained by gusset shaping. (Right) Cross-section of double wall structure in a reentrant cavity.

Lorentz force (or radiation pressure), produced by the EM fields on cavity walls, gives a quadratic detuning: $\delta f \propto -\delta(E_a^2)$. Typical values are a few Hz/(MV/m)^2. This frequency shift can be easily compensated by mechanical tuning once the operation field is reached. However, a large coefficient $\delta f/\delta(E_a^2)$ can generate the so-called ponderomotive oscillations, where small E_a errors, that can be initially induced by any source, cause detuning through Lorentz force and start a self-sustained mechanical vibration [14]. This makes cavity operation difficult and unreliable. Mainly for this reason $df/d(E_a^2)$ should be kept as low as possible, by reinforcing the cavity structure and by means of a careful EM design.

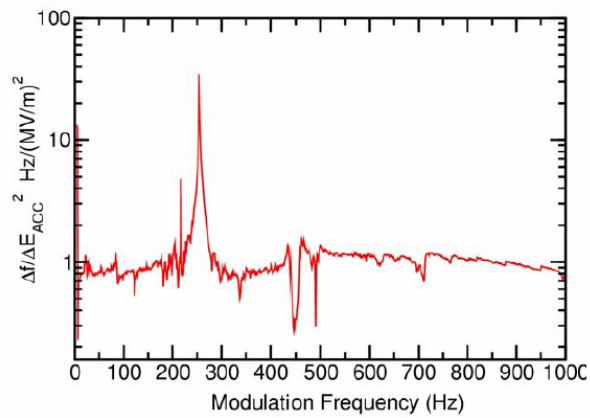

Figure 15. Example of Lorentz force transfer function in a 109 MHz QWR (ANL).

Resonant modes are the most dangerous mechanical instabilities. A small vibration can cause large deformation, and consequently large detuning that can exceed the resonator rf bandwidth. The deformation is usually too fast to be recovered by standard mechanical tuners. After making the detuning range narrower by careful mechanical and rf design, possible solutions to the problem are:

- Widening the rf bandwidth by overcoupling;

- Using fast tuners with suitable range (electronic, piezoelectric, magnetostrictive, electromechanic) [15][16][17];
- Using mechanical dampers [18]
- Using rf damping techniques [19]

Usually the solution requires the combination of many different techniques.

Cavity integration in cryostats. Design objectives are easy installation and maintenance**,** stable and reliable operation. In addition to the usual design requirements of integration of all systems in high vacuum, widely treated during this conference in a dedicated tutorial [20], it should be mentioned that in some low-β cryostats the vacuum volumes inside the resonators (for beam transport) and outside (for thermal isolation) are not separated, but communicating through the beam ports, and pumped out by the same units. In spite of that, high Q can be maintained for years in on-line resonators. The clean resonator apertures are kept closed during assembly, to protect the inner surfaces; during the first pumping out no contamination happen due to the outgoing gas flow. Moreover, dust cannot be transported in vacuum and no contamination happens. However, Q degradation (although usually recoverable with high pressure water rinsing) can appear after the cryostat undergoes venting: dust, deposited on the internal surfaces of the cryostat, is transported inside cavities through beam ports and other apertures. This can be avoided by venting the resonators first, with pure and filtered gas, and maintaining an outgoing flow. This was not always possible in old-design low-β cryostats, but it is being implemented in new ones.

Although common vacuum has some advantages in simplicity and cost, most specialists are still in favour of the well established scheme with separate vacua.

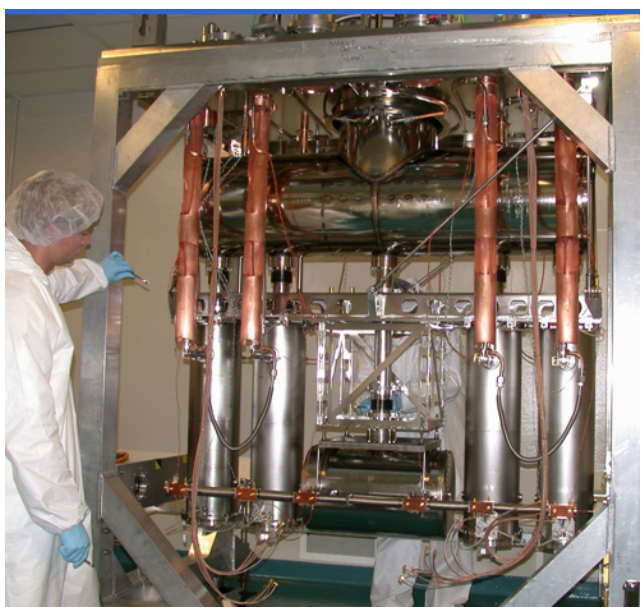

Figure 16. Inner part of a common-vacuum cryostat (TRIUMF ISAC-2) in a clean-room assembly.

Low-β resonators performance. The peak fields of >60 MV/m and >120 mT, achieved in on-line resonators, and residual surface resistance values <1 nΩ achieved in a test cryostat are not very far from the ones achieved by β=1 cavities in similar conditions at 4.2K. This in spite of geometries that are not always favorable for surface preparation (numerous welds, small apertures, etc). On the other hand, the low power dissipation (related to low rf frequency) and the small areas where peak fields are concentrated (related to cavity geometry), facilitate field emission conditioning and the achievement of high gradients. The recent application of the most advanced preparation techniques has raised low-field Q's to very high values.

The frequent appearance of strong Q-slopes that limit the possible operation at high gradient, however, represents one of the main open problems in low-β cavities development.

4. LOW-β CAVITY TYPES AND CHARACTERISTICS

In this paragraph a synthetic review of different low-β resonator families will be given. Families are characterized by the particular EM mode that is excited in the cavities. Only a few references will be given here; for more references and for a recent review of low-β resonators models and performances see, e.g., ref [24].

Quarter-wave structures

The mode excited is a TEM one (Transverse Electric Magnetic) in a λ/4 long transmission line section. This allows to obtain cavities with small g/λ, and relatively small size [25].

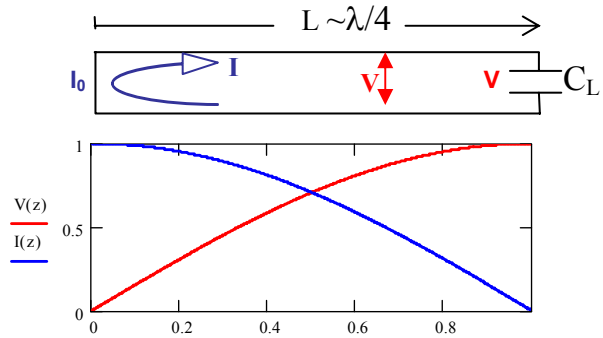

Figure 17. Top: scheme of a quarter-wave structure with loading capacitance. Bottom: Voltage and current amplitude along the line.

Split-ring resonators

. The split ring arms (fig. 19) and the outer conductor wall form a pair of coupled QW transmission lines, with 2 principal modes: push-push (drift tubes at equal voltage) and push-pull (drift tubes at opposite voltage), the latter at lower frequency and used for acceleration [26]. Application range: $90 \le f \le 150$ MHz, $0.05 \le \beta_0 \le 0.15$

"pro" :

- relatively large energy gain

- good efficiency

"contra":

- mechanical stability
- beam steering
- high peak fields
- more expensive and difficult to build than QWRs

Comment: In operation since many years but not developed any longer.

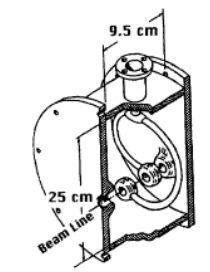

Figure 19. Schematic of a split-ring resonator

Quarter-wave resonators.

Application range: 48≤f≤160 MHz, 0.001≤ β_0≤0.2

"pro" :

- Compact
- Modular
- High performance
- Low cost
- Possibility of large openings, easy access
- Down to very low beta

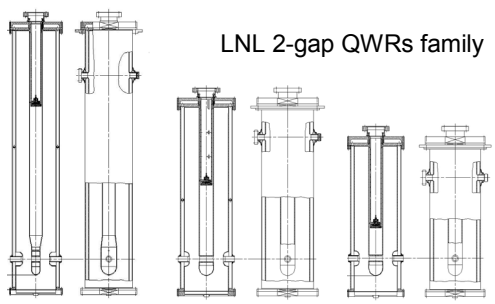

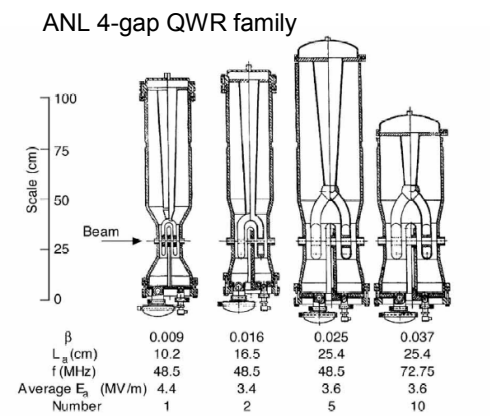

Figure18. Families of 2- and 4-gap QWRs.

"contra":

- Dipole steering above β_0~0.1 (unless corrected)
- Mechanical stability below ~100 MHz

Comment: In operation. Very successful, developed in many models by many laboratories.

Double quarter-wave resonators

Application range: f~225 MHz, β_0 ~0.16

"pro" :

- Most of the pros of QWRs
- Larger voltage gain than 2-gap QWRs

"contra":

- Dipole steering
- Mechanical stability below ~100 MHz

Comment: Originally named "half-wave" for its fundamental mode, with two QWRs operating in push-pull. Prototyped in 1985 for Pb plating and never put in operation [27]. Alternative to Split-ring.

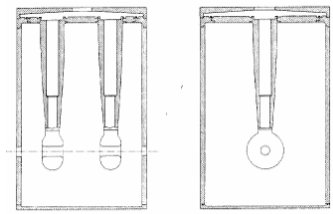

Figure 20. Double QWR schematic.

Half-wave structures

A half-wave structure is equivalent to 2 quarter-wave ones facing each other. The same accelerating voltage of QWRs is obtained with almost 2 times larger power dissipation. The symmetry of the structure, however, cancels steering and allows to use HWRs at higher β than QWRs.

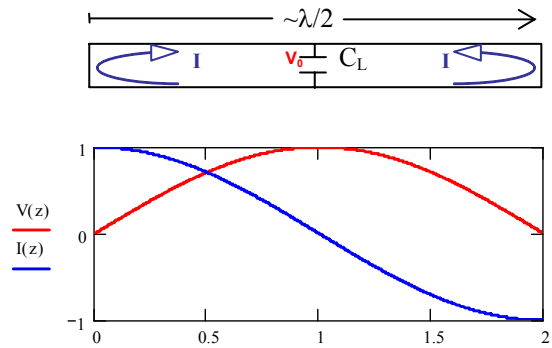

Figure 21. As in Fig. 19, for a half-wave structure.

Half-Wave coaxial resonators

Application range: 160≤f≤352 MHz, 0.09 ≤ β_0≤ 0.3

"pro" :

- No dipole steering
- High performance
- Lower E_p than QWRs
- Very compact

"contra":

- Not easy access

- Difficult to tune
- Less efficient than QWRs

Comment: Prototyped and under production. Best in the frequency range of 160÷250 MHz, too high for QWRs (steering) and too low for SPOKE resonators (large size).

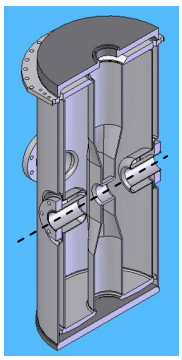


Figure 22. Half-wave coaxial resonators.

Single-SPOKE resonators

Application range: 345≤f≤ 805 MHz, 0.15 ≤ β_0≤ 0.62

"pro" :

- No dipole steering
- High performance
- Higher R_{sh} than HWRs
- Larger aperture than HWRs

"contra":

- Not easy access (but better than HWRs)
- Difficult to tune
- Larger size than HWRs

Comment: Prototyped in many models and β_0, but not yet in operation. Best results around 350÷400 MHz, where it is the most popular choice. Rather large size at lower frequency. Multi-cell possibility.

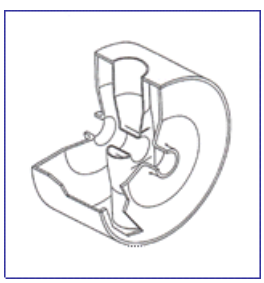


Figure 23. Spoke resonators.

Ladder SC cavities

Application range: 350MHz, 0.1≤ β_0≤ 0.3 [32]

"pro" :

- Efficient
- large energy gain
- They can be made for rather low β
- Easy access

"contra":

- small aperture
- β acceptance
- not easy to build

Comment: Still under development. Multigap cavity with easy access, alternative to CH structures.

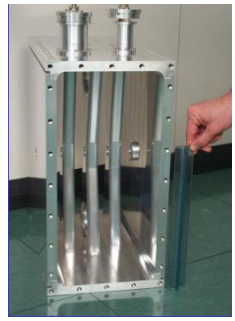

Figure 24. Ladder resonator model.

TM mode cavities

TM010 (Transverse Magnetic) mode: B is always perpendicular to the EM wave propagation axis (and to the beam axis) [2].

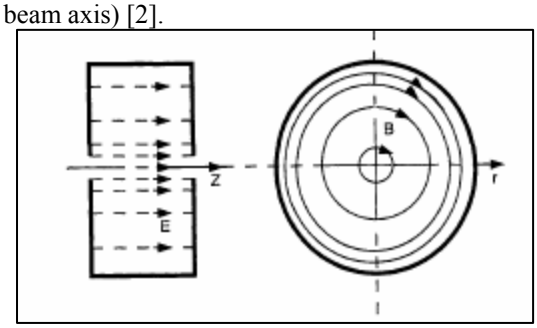

Figure 25. Examples of TM structure: pillbox cavity

Elliptical resonators

Application range: 352≤f≤805 MHz, 0.47≤ β_0≤ 1

"pro" :

- Highly symmetric field
- High performance
- Low E_p and B_p
- Multi cell possibility
- Large aperture

"contra":

- Not suitable for β<0.4
- Mechanical modes

Comment: β_0>0.6 in operation, β_0<0.6 prototyped. Very successful and well developed in many laboratories. Best around 700÷800 MHz.

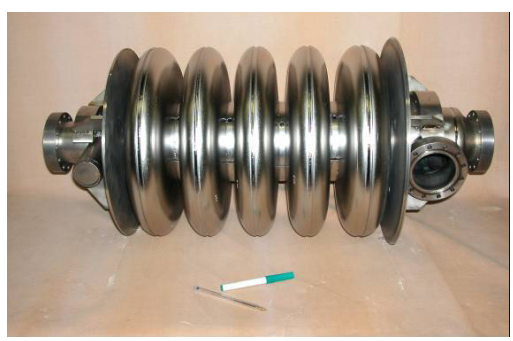

Figure 26. β_0=0.5, 5-cell elliptical resonator.

Reentrant cavities

Application range: 352≤f≤ 402 MHz, 0.1≤ β_0

"pro" :

- Highly symmetric field
- Very Compact
- Low E_p and B_p
- Widest velocity acceptance
- Possibility of large aperture

"contra",

- short accelerating length, little E gain
- mechanical stability
- inductive couplers only

Comment: Prototyped. One of the oldest low-β superconducting cavities [29], recently renewed. For special applications.

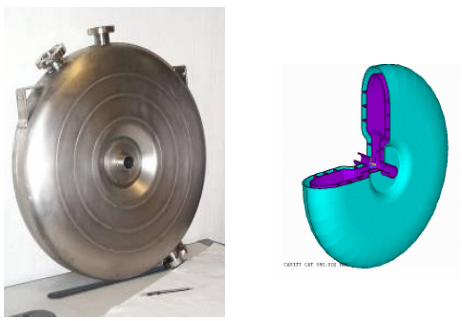

Figure 27. β>0.1 reentrant cavity

IH and CH multi-gap structures

These interdigital and crossed electrode structures have 3 or more gap. The electrodes are either 2 (IH) or 4 (CH) creating dipolar or quadrupolar field distributions, respectively. The magnetic field is parallel to the beam axis. These structures can host either accelerating drift tubes or RFQ electrodes for simultaneous acceleration and focusing at very low-β [30].

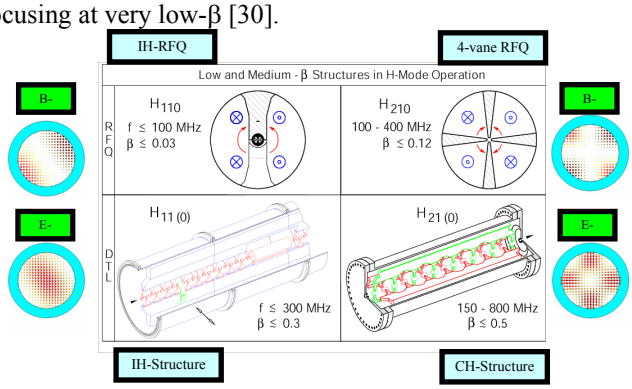

Figure 28. Schematic of IH and CH structures and their application in Drift Tube Linacs and RFQs [30].

Multi-SPOKE resonators

Application range: 345≤f≤ 805 MHz, 0.15≤ β_0≤ 0.62

"pro" :

- High performance
- High efficiency
- Large energy gain
- Lower frequency than elliptical
- Mechanically more stable than elliptical

"contra":

- Large size
- Not easy access
- Difficult to tune
- smaller aperture than elliptical
- More expensive than elliptical

Comment: Prototyped. Very promising, especially around β~0.5, alternative to elliptical cavities. It allows linac lattices with large longitudinal acceptance [31].

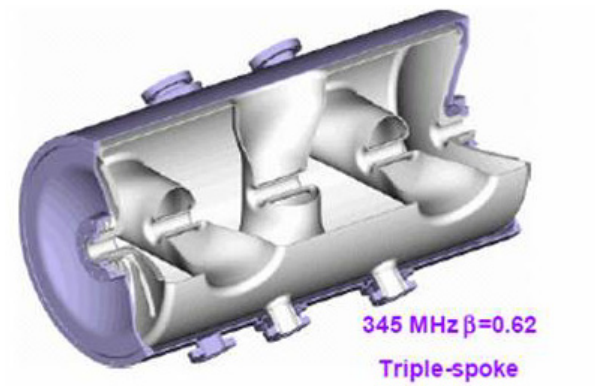

Figure28. Triple-spoke resonator sketch.

CH multi-gap SC cavities

Application range: 174≤f≤ 800 MHz, 0.1≤ β_0≤ 0.3

"pro" :

- Very efficient
- large energy gain
- suitable for rather low β
- It allows a very compact linac

"contra":

- velocity acceptance
- difficult to have large aperture
- not easy to build
- High peak fields
- cost

Comment: Recently prototyped. New technology, very promising for beams with fixed velocity profile.

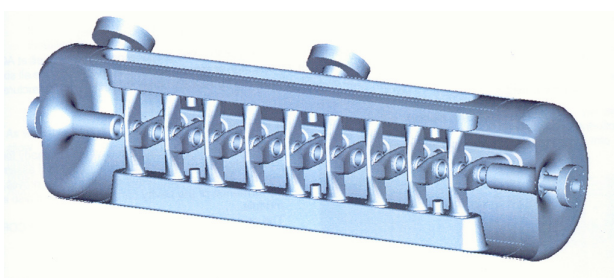

Figure 29. CH 19-gap superconducting resonator.

Superconducting RFQ's

Application range: f~80 MHz, $0.001 \leq \beta_0 \leq 0.035$

"pro" :

- Compact
- CW operation
- High efficiency
- Down to very low beta
- large acceptance

"contra":

- Mechanical stability
- Not easy to build
- MP and FE
- Rather high cost

Comment: In operation. Technologically challenging [33]. Future applications in high power ion linacs could be possible, due to its large aperture and high fields.

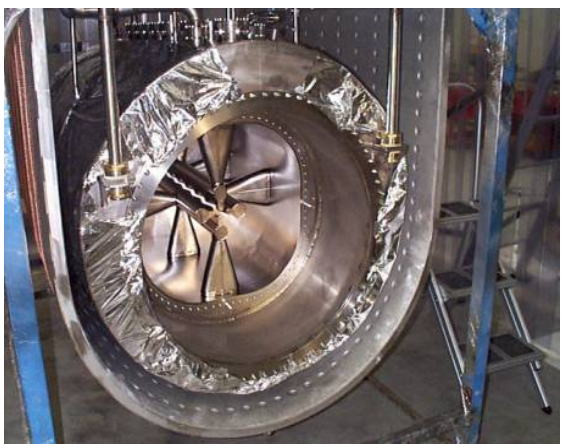

Figure 27. Superconducting RFQ.

FINAL REMARKS

The activity in superconducting low-β resonators development is presently higher than ever before, mainly for the new proposed applications in high power linacs and in radioactive beams post-accelerators. Very good perfomances have been achieved. Only recently, the very successful technology of Nb treatment developed for β=1 cavities was fully exploited in low-β ones, and performances are expected to improve further. Numerous projects, some of them funded, foresee a large variety of low-β resonators. There are different models of cavities developed for the same application; we will be able soon to evaulate and compare the results to find optimal choices. There are still problems not completely solved, like Q-slope and cures for mechanical instability. New ideas and new inventions will be needed to fulfill all requirements.

REFERENCES

[1] S. Belomestnykh and V. Shemelin, "High-beta cavity design", these proceedings.

[2] T. Wangler, "Rf linear accelerators" (Wiley).

[3] J.Delayen, "Low and Intermediate Beta Cavity Design – a Tutorial", proc. of SRF03.

[4] H.Padamsee, J. Knobloch and T. Hays, "Rf superconductivity for accelerators" (Wiley).

[5] K. Saito, "Basic Principles of SRF", these proceedings.

[6] A. Porcellato, "Niobium sputtered QW resonators", these preoceedings.

[7] W. Moeller, "Input couplers for superconducting cavities - design and test", these proceedings.

[8] F.L. Krawczic, "Cavity and Power Coupler Integration", Workshop on High-Power Couplers for Superconducting Accelerators, Jefferson Lab, Newport News, Virginia, 2002.

[9] R.L. Geng, "Multipacting Simulations for Superconducting Cavities and RF Coupler Waveguides", Proc. of the 2003 Particle Accelerator Conference.

[10] A. Facco, V. Zviagintsev, "Study on Beam Steering in Intermediate-β Superconducting Quarter-wave Resonators", Proceedings of the 2001 Particle Accelerator Conference, Chicago

[11] P.N. Ostroumov, K.W. Shepard, Physical Review Special Topics - Accelerators and Beams, vol. 4, 110101, 2001.

[12] Brian Rusnak, "RF Power and HOM Coupler Tutorial", proc. of SRF03.

[13] K. W. Shepard, M. Kedzie, and M. P. Kelly, T. Schultheiss, "Superconducting Intermediate-Velocity Drift-tube Cavities for the RIA Driver Linac", Proceedings of the 2001 Particle Accelerator Conference, Chicago.

[14] J. Delayen, "Ponderomotive instabilities and microphonics", these proceedings.

[15] N.Added, B.E.Clifft and K.W.Shepard, "Upgraded Phase Control System For Superconducting Low-Velocity Accelerating Structures" Proc. of 16th LINAC Conf., August 24-28, 1992, Ottawa, Ontario.

[16] P. Sekalski, S. Simrock, A. Napieralski, "Piezoelectric stack based system for Lorentz force compensation", these proceedings.

[17] T.Ries, K. Fong, S. Koscielniak, R.E. Laxdal, G. Stanford, "A Mechanical Tuner for the ISAC-II Quarter Wave Superconducting Cavities", Proceedings of the 2003 Particle Accelerator Conference.

[18] A. Facco, "Mechanical mode damping in superconducting low-β resonators", Particle Accelerators, Vol. 61, 1998, pp. 265-278.

[19] J. R. Delayen, "Electronic Damping of Microphonics in Superconducting Cavities", Proc. of the 2001 Particle Accelerator Conference, Chicago.

[20] C. Pagani, "Cryomodule design, assembly, alignment", these proceedings.

[21] E. Palmieri, "Advancement in comprehension of the Q-slope for superconducting cavities", these proceedings.

[22] J. Halbritter, "The Nb-oxide system", these proceedings.

[23] G. Eremeev, "New results on "high-field Q-slope"", these proceedings.

[24] A. Facco, "Low and Medium Beta Superconducting Cavities", Proc. of EPAC '04, Lucerne, Switzerland, 2004.
[25] I. Ben-Zvi and J.M. Brennan,Nucl. Instr. And Meth. 212 (1983) 73.
[26] K.W.Shepard, J.E.Mercereau, and G.J.Dick, IEEE Trans. Nucl. Sci. NS-22, 1179 (1975).
[27] J. R. Delayen, "Superconducting Accelerating Structures for High-Current Ion Beams," Proc. LINAC'88, Newport News, October 1988, p. 199.
[28] M.P. Kelly, K.W. Shepard, M. Kedzie, G. Zinkann, in Proc. 2001 Particle Accelerator Conf., June 18-22, 2001, Chicago, IL (2001), p. 1047.
[29] P.H. Ceperly, J.S. Sokolowski, I. Ben-Zvi, H.F. Glavish and S.S. Hanna, "Beam test of a superconducting niobium cavity for a heavy ion accelerator", Nuclear Instruments and Methods136 (1976) 421-423.
[30] R. Eichhorn and U. Ratzinger, "Superconducting H-mode Structures for Medium Energy Beams", Proc.of the XX International Linac Conference, Monterey, California,2000.
[31] K.W. Shepard, P. N. Ostroumov, J. R. Delayen, "High-energy ion linacs based on superconducting spoke cavities", PHYSICAL REVIEW SPECIAL TOPICS - ACCELERATORS AND BEAMS, VOLUME 6, 080101 (2003).
[32] V. Andreev et al., "Study of a Novel Superconducting Structure for the Very Low Beta Part of High Current Linacs", Proc. of EPAC 2002, Paris, France, 2002.
[33] G. Bisoffi et al., "Superconducting RFQ", Proc. of SRF2001, Tsukuba, Japan, 2003.